ICSV13 - Vienna
The Thirteenth International Congress on Sound and Vibration
Vienna, Austria, July 2-6, 2006

WAVE PROPAGATION BEHAVIOR OF A MULTI-CONNECTED STRUCTURE

Akemi Nishida*

*Center for Computational Science and E-system, Japan Atomic Energy Agency
6-9-3, Higashiueno, Taito-ku, Tokyo 110-0015, JAPAN
nishida.akemi@jaea.go.jp

Abstract

It is crucial to continuously maintain safety and functionality in a nuclear plant. In particular, in response to the recent piping damage accident, the necessity for detailed analysis has increased. Thus, frame structures, such as piping, are gaining in importance with regard to modeling, which can reproduce the real phenomenon. So far, the author has continuously researched stress wave propagation in frame structures in order to clarify the wave propagation behavior of non-periodic and complicated assembled structures. A spectrum element method (SEM) has been adopted as one of the effective methods, and its application to a real-sized structure is desired. When carrying out simulation of the wave propagation phenomenon to target the transient response, it was found that the frame element in SEM was required to be adopted by considering the shear and torsional deformations. Here, as the first step for the stress wave propagation simulation of the piping structure used in a nuclear plant, a simulation was attempted for a multi-connected frame structure where some components were joined.

INTRODUCTION

Generally, it is difficult to predict the occurrence of natural disasters such as earthquakes, tsunamis, and typhoons. Therefore, a performance management system that constantly maintains the safety and functionality of structures is required, particularly for critical structures like nuclear power plants. In order to realize such a system, it is becoming important to carry out detailed modeling procedures and analyses to better understand actual phenomena. Such details are important in understanding the phenomena occurring in frame structures such as piping systems, which are considered to be among the weakest and most vulnerable components of nuclear power plants. Nuclear power plant accidents such as the fractures caused by fluid elastic vibration in small tubes used for heat transfer from the steam generators and cracks in the welded parts of the piping caused by cyclic stress of the piping vibration, have been recently reported. The clarification of the dynamic behavior of the piping structure during operation is urgently required in order to avoid these accidents. The aim of our research is to determine the dynamic behavior—especially the wave propagation phenomena under impulsive load—of piping systems in nuclear power plants, which are complicated assemblages of parts.

The elastic wave theory has been primarily used to investigate the response of a structure subjected to an impact load in a structural field. The Laplace transformation is generally used to analyze the wave equation, which is expressed by a partial differential equation. However, it is not easy to analytically perform the inverse transformation for the solution in the frequency domain, except in some special cases. Due to this difficulty, many approximate methods have been proposed (For example, Refs.[1] and [2]). On the other hand, Krings et al.[3] changed the equation of the Laplace inverse transformation such that the fast Fourier transformation (FFT) algorithm could be used. Doyle[4] proposed another method that uses Fourier transformation instead of Laplace transformation and showed that the method is applicable to the analysis of structures with multi-degrees of freedom. This analytical method is called the spectral element method and has an advantage with regard to the ability to use the FFT algorithm. Nishida et al.[6][7] developed this method for three-dimensional frame structures with shear and torsional effects. By using this method, a multi-connected frame model with infinite boundaries is analyzed and compared with the experimental results in this paper. As the results, the applicability of the presented element is shown.

SPECTRAL ANALYSIS OF WAVE MOTION IN FRAME STRUCTURES

Governing equations for a frame

Let us consider a homogeneous, isotropic, linear, and elastic frame. The *x*-axis coincides with the neutral axis of the frame that passes through the centroid of the cross section. The *y*- and *z*-axis lie in the plane of the neutral surface of the frame and coincide with the principal axes of the cross section. The displacements, rotational angles, resultant forces, and moments in each direction are represented by $u_l,\ \theta_l,\ P_l$, and $M_l\ \left(l = x, y, z\right)$, respectively. The basic hypothesis of one-dimensional wave theory is used for longitudinal and torsional motions; and the Timoshenko beam theory, for flexural motions. The Timoshenko beam theory is sufficiently accurate to represent wave propagation behavior including bending and shear deformation[5]. As a result, the governing equations for the frame assume the following form:

$$\frac{\partial^2 u_x}{\partial x^2} - \frac{1}{C_0^{\,2}}\frac{\partial^2 u_x}{\partial t^2} = 0 \tag{1.1}$$

$$\frac{\partial^2 \theta_x}{\partial x^2} - \frac{1}{C_2^{\,2}}\frac{\partial^2 \theta_x}{\partial t^2} = 0 \tag{1.2}$$

$$c_{sy}{}^2\left[\frac{\partial^2 u_y}{\partial x^2}-\frac{\partial \theta_z}{\partial x}\right]=\frac{\partial^2 u_y}{\partial t^2} \tag{1.3}$$

$$\left(c_0 q\right)_y{}^2\frac{\partial^2 \theta_z}{\partial x^2}+c_{sy}{}^2\left[\frac{\partial u_y}{\partial x}-\theta_z\right]=Q_y{}^2\frac{\partial^2 \theta_z}{\partial t^2} \tag{1.4}$$

$$c_{sz}{}^2\left[\frac{\partial^2 u_z}{\partial x^2}-\frac{\partial \theta_y}{\partial x}\right]=\frac{\partial^2 u_z}{\partial t^2} \tag{1.5}$$

$$\left(c_0 q\right)_z{}^2\frac{\partial^2 \theta_y}{\partial x^2}+c_{sz}{}^2\left[\frac{\partial u_z}{\partial x}-\theta_y\right]=Q_z{}^2\frac{\partial^2 \theta_y}{\partial t^2} \tag{1.6}$$

where

$$C_0=\frac{E}{\rho},\ C_2=\frac{G}{\rho}$$

$$\left(c_0 q\right)_y{}^2=\frac{EI_z}{\rho A},\ c_{sy}{}^2=\frac{\left(GAK\right)_y}{\rho A},\ \mathrm{Q}_y{}^2=\frac{\rho I_z}{\rho A}$$

$$\left(c_0 q\right)_z{}^2=\frac{EI_y}{\rho A},\ c_{sz}{}^2=\frac{\left(GAK\right)_z}{\rho A},\ \mathrm{Q}_z{}^2=\frac{\rho I_y}{\rho A}$$

and E is Young's modulus, G is the shear modulus, ρ is the mass density, A is the cross sectional area, I_y and I_z are the moments of inertia with respect to the *y*- and *z*-axis, respectively, and J is the polar moment of inertia. The resultant forces and moments in each direction are given as follows:

$$P_x=EA\frac{\partial u_x}{\partial x}$$

$$P_y=\left(GAK\right)_y\left[\frac{\partial u_y}{\partial x}-\theta_z\right]=-EI_z\frac{\partial^2 \theta_z}{\partial x^2}+\rho I_z\frac{\partial^2 \theta_z}{\partial t^2}$$

$$P_z=\left(GAK\right)_z\left[\frac{\partial u_z}{\partial x}-\theta_y\right]=-EI_y\frac{\partial^2 \theta_y}{\partial x^2}+\rho I_y\frac{\partial^2 \theta_y}{\partial t^2}$$

$$M_x=GJ\frac{\partial \theta_x}{\partial x},\ M_y=-EI_y\frac{\partial \theta_y}{\partial x},\ M_z=EI_z\frac{\partial \theta_z}{\partial x}$$

The shear and bending stiffness are governed by GAK and EI, respectively, while the corresponding inertias are ρA and ρI.

Spectral analysis

To obtain the general solution for Equation (1), spectral analysis is performed. Then, the general displacements and rotational angles can be represented as follows:

$$\begin{aligned}
u_x(x,t)&=\sum \hat{u}_x(x,\omega)\exp[i\omega t]\\
u_y(x,t)&=\sum \hat{u}_y(x,\omega)\exp[i\omega t]\\
u_z(x,t)&=\sum \hat{u}_z(x,\omega)\exp[i\omega t]\\
\theta_x(x,t)&=\sum \hat{\theta}_x(x,\omega)\exp[i\omega t]\\
\theta_y(x,t)&=\sum \hat{\theta}_y(x,\omega)\exp[i\omega t]\\
\theta_z(x,t)&=\sum \hat{\theta}_z(x,\omega)\exp[i\omega t]
\end{aligned} \tag{2}$$

Local stiffness matrix of a finite length spectral element

Consider a three-dimensional frame element of length L, as shown in Figure 1. Using the general solutions represented by Equation (2), the displacement shape functions for the spectral element can be represented by

$$\hat{u}_x(x,\omega) = A_1 \exp\left[-ik_0 x\right] + A_2 \exp\left[-ik_0(L-x)\right] \tag{3.1}$$

$$\hat{\theta}_x(x,\omega) = B_1 \exp\left[-ik_2 x\right] + B_2 \exp\left[-ik_2(L-x)\right] \tag{3.2}$$

$$\begin{aligned}\hat{u}_y(x,\omega) &= P_{1y}\bar{C}_1 \exp\left[-ik_{1y}x\right] + P_{2y}\bar{C}_2 \exp\left[-ik_{2y}x\right] \\ &\quad + P_{3y}\bar{C}_3 \exp\left[-ik_{1y}(L-x)\right] + P_{4y}\bar{C}_4 \exp\left[-ik_{2y}(L-x)\right]\end{aligned} \tag{3.3}$$

$$\begin{aligned}\hat{\theta}_z(x,\omega) &= \bar{C}_1 \exp\left[-ik_{1y}x\right] + \bar{C}_2 \exp\left[-ik_{2y}x\right] \\ &\quad + \bar{C}_3 \exp\left[-ik_{1y}(L-x)\right] + \bar{C}_4 \exp\left[-ik_{2y}(L-x)\right]\end{aligned} \tag{3.4}$$

$$\begin{aligned}\hat{u}_z(x,\omega) &= P_{1z}\bar{D}_1 \exp\left[-ik_{1z}x\right] + P_{2z}\bar{D}_2 \exp\left[-ik_{2z}x\right] \\ &\quad + P_{3z}\bar{D}_3 \exp\left[-ik_{1z}(L-x)\right] + P_{4z}\bar{D}_4 \exp\left[-ik_{2z}(L-x)\right]\end{aligned} \tag{3.5}$$

$$\begin{aligned}\hat{\theta}_y(x,\omega) &= \bar{D}_1 \exp\left[-ik_{1z}x\right] + \bar{D}_2 \exp\left[-ik_{2z}x\right] \\ &\quad + \bar{D}_3 \exp\left[-ik_{1z}(L-x)\right] + \bar{D}_4 \exp\left[-ik_{2z}(L-x)\right]\end{aligned} \tag{3.6}$$

where

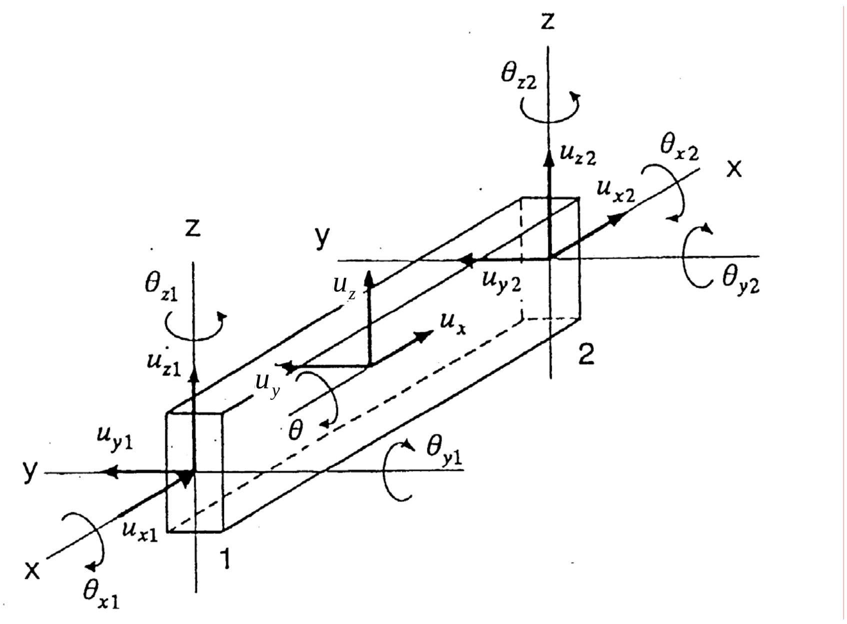

Figure 1 – Three-dimensional finite frame element

$$k_0 = \omega\sqrt{\frac{\rho}{E}},\ k_2 = \omega\sqrt{\frac{\rho}{G}},$$

$$k_{1y},\ k_{2y} = \left\{\frac{1}{2}\left[\left(\frac{1}{c_{sy}}\right)^2 + \left(\frac{Q_y}{(c_0 q)_y}\right)^2\right]\omega^2 \pm \sqrt{\left(\frac{\omega}{(c_0 q)_y}\right)^2 + \frac{1}{4}\left[\left(\frac{1}{c_{sy}}\right)^2 - \left(\frac{Q_y}{(c_0 q)_y}\right)^2\right]^2 \omega^4}\right\}^{\frac{1}{2}}$$

$$k_{1z},\ k_{2z} = \left\{\frac{1}{2}\left[\left(\frac{1}{c_{sz}}\right)^2 + \left(\frac{Q_z}{(c_0 q)_z}\right)^2\right]\omega^2 \pm \sqrt{\left(\frac{\omega}{(c_0 q)_z}\right)^2 + \frac{1}{4}\left[\left(\frac{1}{c_{sz}}\right)^2 - \left(\frac{Q_z}{(c_0 q)_z}\right)^2\right]^2 \omega^4}\right\}^{\frac{1}{2}}$$

$$P_{1y} = \frac{ik_{1y}}{k_{1y}{}^2 - \omega^2/c_{sy}{}^2},\ P_{2y} = \frac{ik_{2y}}{k_{2y}{}^2 - \omega^2/c_{sy}{}^2}$$

$$P_{3y} = \frac{-ik_{1y}}{k_{1y}{}^2 - \omega^2/c_{sy}{}^2} = -P_{1y},\ P_{4y} = \frac{-ik_{2y}}{k_{2y}{}^2 - \omega^2/c_{sy}{}^2} = -P_{2y}$$

$$P_{1z} = \frac{ik_{1z}}{k_{1z}{}^2 - \omega^2/c_{sz}{}^2},\ P_{2z} = \frac{ik_{2z}}{k_{2z}{}^2 - \omega^2/c_{sz}{}^2}$$

$$P_{3z} = \frac{-ik_{1z}}{k_{1z}{}^2 - \omega^2/c_{sz}{}^2} = -P_{1z},\ P_{4z} = \frac{-ik_{2z}}{k_{2z}{}^2 - \omega^2/c_{sz}{}^2} = -P_{2z}$$

Let us denote the nodal displacements and forces at node 1 ($x = 0$) and node 2 ($x = L$) in the frequency domain by index subscripts 1 and 2, respectively. Using the condition that the displacements and forces at $x = 0$ and $x = L$ are equal to the nodal displacements and forces, the unknown coefficients $A_i, B_i\,(i = 1, 2)$ and $\bar{C}_i,\ \bar{D}_i\,(i = 1, 2, 3, 4)$ can be evaluated. After evaluating the element stiffness matrix for all the elements, the procedure of the conventional matrix method can be used to obtain the solution. However, in this case, it is necessary to compute the solution for all divided discrete frequencies. By the application of inverse fast Fourier transformation (IFFT) to the computed solution, we can obtain the solution in the time domain.

The stabilization of numerical computation can be achieved through the insertion of some semi-infinite elements into the structure to be analysed[7]; these elements create a damping effect. Further, the use of the same method requires an analysis to be carried out on only a part of the large structure.

COMPARISON OF EXPERIMENT RESULTS AND ANALYSIS RESULTS

To investigate the applicability of the presented element, a multi-connected frame model with infinite boundaries was analyzed and compared with the experimental results shown in the reference [8]. The experimental model and its setup are shown in Figure 2 and Photograph 1, respectively. The analytical model is shown in Figure 3. The load history recorded in the experiment was used as the input load for the analytical model (Figure 4).

The moment histories at point No.2, obtained by experiment and analysis are shown in Figure 5. The global behavior of each result is similar, and the maximum amplitude of the moment is almost the same. On the other hand, the phase of each history is slightly different. The main reason for this seems to be that the boundary conditions of the analytical model—assumed as infinite elements—differ in the real conditions.

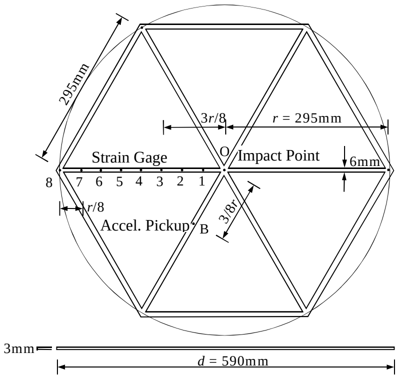

Figure 2 – The experimental model

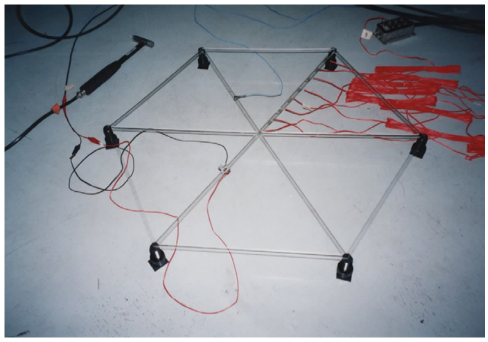

Photograph 1 – Setup of the experimental model

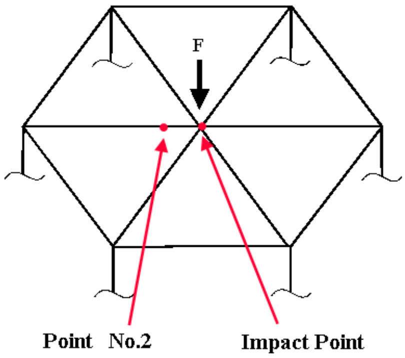

Figure 3 – The analytical model

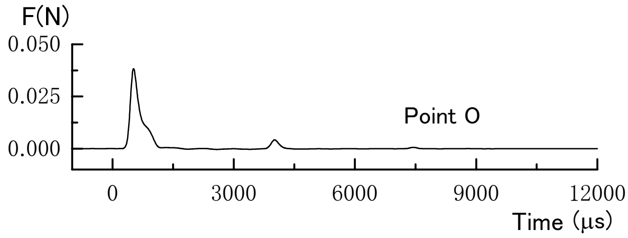

Figure 4 – Force history at the center

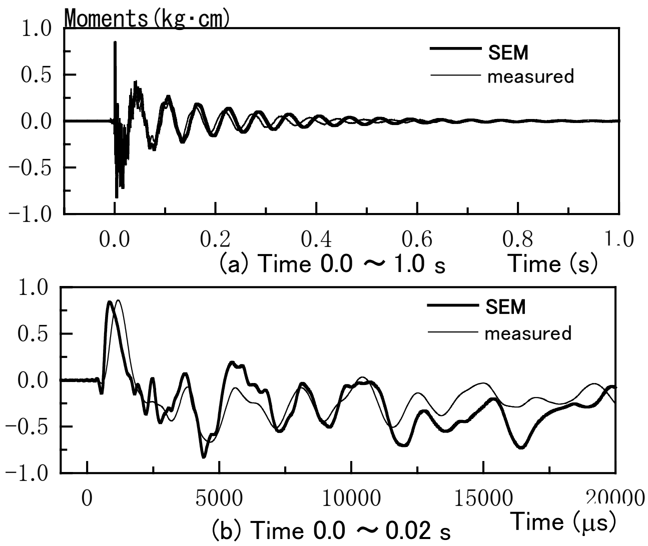

Figure 5 – The moment histories at point 2

CONCLUSION

The application of the wave propagation analytical method for a multi-connected frame structure was shown in this paper. The results were compared with the experimental results. It was found that the presented element could effectively represent the wave propagation phenomena and that the modeling of the boundary condition was crucial for estimating the phase properties of a multi-connected frame structure. As a topic for future study, we are preparing to conduct the numerical simulation of the piping system in a real nuclear reactor system.

REFERENCES

[1] Davies, B. and Martin, B., "Numerical Inversion of the Laplace Transform: A Survey and Comparison of Methods", J. Comput. Phys., 33, 1-32 (1979).

[2] Wilcox, D.J. and Gibson, I.S., "Numerical Laplace Transformation and Inversion in the Analysis of Physical Systems", Int. J. Num. Eng., 20, 8, 1507-1519 (1984).

[3] Krings, W. and Waller, H., "Contribution to the Numerical Treatment of Partial Differential Equations with the Laplace Transformation—An Application of the Algorithm of the Fast Fourier Transformation", Int. J. Num. Meth. Eng., 14, 1183–1196 (1979).

[4] Doyle, J.F., Wave Propagation in Structures—An FFT-based Spectral Analysis Methodology. (Springer-Verlag, 1989).

[5] Gopalakrishnan, S., Martin, M. and Doyle, J.F., "A Matrix Methodology for Spectral Analysis of Wave Propagation in Multiple Connected Timoshenko Beams", Journal of Sound and Vibration, 158, 1, 11-24 (1992).

[6] Nishida, A. and Hangai, Y., "Wave Propagation Behavior of Spatial Structures: Impact Response Analysis of Single Layer Lattice Domes", International Journal of Space Structures, 12, 3/4, 225-237 (1997).

[7] Nishida, A., "Wave Propagation Properties of Frame Structures —Formulation for Three-dimensional Frame Structures", JSME International Journal, B, Special Issue of ICOPE-05 & ICONE2005 (2006) (in print).

[8] Liu, Peng, Nishida, A. and K, Kawaguchi, "Wave Propagation Experiment and DSM Analysis of Planar Lattice Structures Consisting of Triangular Units", Summaries of Technical Papers of Annual Meeting, AIJ, Structural Issue B-1, 813-814 (2001).